

1 **A new high-quality genome assembly and annotation for the threatened Florida Scrub-Jay**
2 (*Aphelocoma coerulescens*)

3 Faye G. Romero^{1*}, Felix E.G. Beaudry^{1,2}, Eyvind Hovmand Warner¹, Tram N. Nguyen³, John
4 W. Fitzpatrick^{3,4}, Nancy Chen¹

5

6 ¹Department of Biology, University of Rochester. Rochester, NY, USA.

7 ²Ontario Institute for Cancer Research. Toronto, ON, Canada.

8 ³Department of Ecology & Evolutionary Biology, Cornell University. Ithaca, NY, USA.

9 ⁴Cornell Lab of Ornithology, Cornell University. Ithaca, NY, USA.

10

11 ¹402 Hutchison Hall. Rochester, NY 14620.

12 ²MaRS Centre. 661 University Avenue, Suite 510. Toronto, Ontario Canada, M5G 0A3

13 ³E145 Corson Hall. Ithaca, NY 14853.

14 ⁴159 Sapsucker Woods Rd. Ithaca, NY 14850.

15

16 *Corresponding author: fromero3@ur.rochester.edu

17

18 Keywords: Florida Scrub-Jay, Corvidae, de novo genome assembly, linkage map, pedigree

19

20 **ABSTRACT**

21 The Florida Scrub-Jay (*Aphelocoma coerulescens*), a Federally Threatened,
22 cooperatively-breeding bird, is an emerging model system in evolutionary biology and ecology.
23 Extensive individual-based monitoring and genetic sampling for decades has yielded a wealth of

24 data, allowing for the detailed study of social behavior, demography, and population genetics of
25 this natural population. Here, we report a linkage map and a chromosome-level genome
26 assembly and annotation for a female Florida Scrub-Jay made with long-read sequencing
27 technology, chromatin conformation data, and the linkage map. We constructed a linkage map
28 comprising 4,468 SNPs that had 34 linkage groups and a total sex-averaged autosomal genetic
29 map length of 2446.78 cM. The new genome assembly is 1.32 Gb in length, consisting of 33
30 complete or near-complete autosomes and the sex chromosomes (ZW). This highly contiguous
31 assembly has an N50 of 68 Mb and a Benchmarking Universal Single-Copy Orthologs (BUSCO)
32 completeness score of 97.1% with respect to the *Aves* database. The annotated gene set has a
33 BUSCO transcriptome completeness score of 95.5% and 18,051 identified protein-coding genes,
34 92.2% of which have associated functional annotations. This new, high-quality genome assembly
35 and linkage map of the Florida Scrub-Jay provides valuable tools for future research into the
36 evolutionary dynamics of small, natural populations of conservation concern.

37

38 **ARTICLE SUMMARY**

39 We present a new high-quality genome assembly and annotation for the Florida Scrub-
40 Jay (*Aphelocoma coerulescens*), a Federally Threatened bird species. In comparison to other
41 genome assemblies of this species, our assembly is the first to be made using long-read
42 sequencing technology and is the first generated from a female individual. We also constructed
43 the first linkage map for this species using a population pedigree. Our genome assembly is highly
44 contiguous and is of similar quality to other bird genome assemblies.

45

46 **INTRODUCTION**

47 The Florida Scrub-Jay (*Aphelocoma coerulescens*) is a Federally Threatened,
48 cooperatively-breeding bird endemic to the U.S. state of Florida (Figure 1A) (Woolfenden and
49 Fitzpatrick 1984). This species has been in decline due to anthropogenic development and fire
50 suppression, and currently exists in small, locally isolated populations across the state (Boughton
51 and Bowman 2011). The Florida Scrub-Jay is intensively monitored throughout its range with
52 several well-characterized natural populations, including a long-term study at Archbold
53 Biological Station in Venus, FL. All individuals in this population have been uniquely banded
54 and monitored since 1969, resulting in a 16-generation pedigree with near-complete fitness data
55 (Figure 1B) (Woolfenden and Fitzpatrick 1984). This robust dataset has led to foundational
56 knowledge in the behavior, demography, and life history of cooperative breeders (Woolfenden
57 and Fitzpatrick 1984), with further work shedding light on social and environmental effects on
58 lifetime fitness (Mumme *et al.* 2015) and the causes and consequences of dispersal and
59 immigration (Coulon *et al.* 2010; Aguillon *et al.* 2017; Suh *et al.* 2020, 2022; Summers *et al.*
60 2024). Studies of other populations of Florida Scrub-Jays have contributed to our understanding
61 of the negative impacts of suburbanization (Thorington and Bowman 2003; Coulon *et al.* 2012),
62 population dynamics (Breininger *et al.* 1999; Breininger and Carter 2003), and the repercussions
63 of translocations (Linderroth *et al.* 2023). Exhaustive genetic sampling of thousands of
64 individuals at Archbold Biological Station has also allowed for the rare opportunity to study the
65 evolution of small, natural populations, such as genetic population structure (Coulon *et al.* 2008,
66 2010), allele frequency changes (Chen *et al.* 2019), and the genetic consequences of inbreeding
67 and reduced immigration (Chen *et al.* 2016; Nguyen *et al.* 2022), all of which are imperative to
68 understand in the face of habitat fragmentation and the loss of genetic diversity in species

69 worldwide (Thomas *et al.* 2004). To better characterize the genetic variation present in the
70 Florida Scrub-Jay, we must have a high-quality reference genome as a point of comparison.

71 A reference genome for a male Florida Scrub-Jay was published as part of the Bird
72 10,000 Genomes Project (version 1; v1) (Feng *et al.* 2020) and was further improved and
73 scaffolded with the aid of Hi-C reads (version 2; v2) (Driscoll & Beaudry, *et al.* 2021). However,
74 these assemblies were generated with Illumina short-read data, which may not have captured the
75 full scope of genomic information, such as highly repetitive regions (Treangen and Salzberg
76 2012). Additionally, as birds have a ZW sex-determination system in which females are the
77 heterogametic sex, these assemblies are missing the W chromosome. Here, we present a new
78 chromosome-level genome assembly for a female Florida Scrub-Jay generated with long-read
79 sequencing technology, chromosome conformation data, and a linkage map. The version 3 (v3)
80 assembly, which is 1.32 Gb long, adds 260 Mb in length to the previous reference genomes and
81 contains 4 newly identified chromosomes to the Florida Scrub-Jay, including the W
82 chromosome. We also provide annotations of repetitive and gene content, evaluations of the
83 quality and contiguity of the data presented, and the first linkage map for this species.

84

85 MATERIALS AND METHODS

86 Sampling and genome sequencing

87 We collected fresh blood via venipuncture from an inbred, adult female Florida Scrub-
88 Jay at Archbold Biological Station, Venus, FL (approved by Cornell University Institutional
89 Animal Care and Use Committee (IACUC 2010-0015), authorized by permit no. TE824723-8
90 issued by the US Fish and Wildlife Service, banding permit no. 07732 issued by the US
91 Geological Survey, and permit no. LSSC-10-00205 issued by the Florida Fish and Wildlife

92 Commission). The University of Delaware DNA Sequencing & Genotyping Center extracted
93 DNA from the blood sample using a High Molecular Weight extraction protocol, then prepared a
94 Pacific Biosciences (PacBio) library and sequenced it on 3 SMRT Cells (Sequel IIe system).

95 We also performed 20x coverage whole-genome resequencing for 25 males and 25
96 female Florida Scrub-Jays, including the parents of the individual we sampled for PacBio
97 sequencing. We extracted DNA from archived blood samples stored in Queen's lysis buffer
98 using Qiagen DNeasy Blood and Tissue kits and sent DNA to Novogene (Sacramento, CA,
99 USA) for PCR-free library preparation and 150 bp paired-end sequencing on an Illumina
100 NovaSeq6000 platform.

101

102 Linkage map generation

103 We created a linkage map using CRI-MAP v. 2.507 (Green *et al.* 1990) and the CRIGEN
104 package (Liu and Grosz 2006). We used data from a previous study that genotyped 3,838
105 individuals at 12,210 SNPs using a custom Illumina iSelect Beadchip (Chen *et al.* 2016). We
106 trimmed our pedigree to include only completely genotyped trios, then split it into 32 three-
107 generation sub-families of ~100 individuals each using the *crigen* function. Using a subset of
108 3,424 informative SNPs (1 SNP per scaffold of Florida Scrub-Jay genome v1; Feng *et al.* 2020),
109 we created a sparse (pre-framework) map. We calculated pairwise LOD scores using *twopoint*
110 and assigned markers to linkage groups using the *autogroup* function. *Autogroup* uses an
111 iterative process to assign markers to linkage groups with four levels of increasing stringency.
112 The parameters we used for minimum LOD score, minimum number of informative meioses,
113 maximum number of shared linkages, and minimum linkage ratio were: level 1 (100, 2.0, 2, 0.9),
114 level 2 (50, 1.5, 3, 0.7), level 3 (10, 1.0, 5, 0.6), and level 4 (5, 0.4, 6, 0.5). We labelled linkage

115 groups based on alignments with the Zebra finch genome (NCBI accession: GCA_000151805.2).

116 Then, to construct each linkage group, we identified haplogroups using the *hap* function and ran

117 *build* four times with different starting markers and a threshold of $LOD > 5$. We chose the

118 longest map as the pre-framework map for each linkage group. To check marker order, we

119 permuted up to five adjacent markers with the function *flips* to look for alternative marker orders

120 with higher likelihood and iteratively updated the marker order until no better orders were found.

121 To expand the pre-framework map, we ran *twopoint* and *autogroup* on the full SNP set as

122 above to assign the remaining markers to linkage groups. For each linkage group, we added

123 markers onto the pre-framework map using *build* with a threshold of $LOD > 5$ and confirmed

124 marker order with *flips*. For three linkage groups (LG 34, 36, and chr Z), we added additional

125 markers using *build* with a threshold of $LOD > 3$ and checked marker order with *flips*. When

126 linkage groups had multiple equivalent best orders, we either removed markers with multiple

127 potential orders or picked the order that was most consistent with the physical map. Finally, we

128 used *fixed* to output the maximum likelihood recombination fractions and map distances for the

129 sex-averaged map (setting SEX_EQ to 1) and the sex-specific map (setting SEX_EQ to 0). We

130 used crimaptools v0.1 (<https://github.com/susjoh/crimaptools>, (Johnston *et al.* 2016)) to parse

131 output files.

132

133 De novo genome assembly

134 To assemble the genome, we first used Cutadapt v. 2.3 (Martin 2011) to identify and

135 discard PacBio HiFi raw reads with adapter sequences. Next, we created primary and alternate

136 draft assemblies using hifiasm v. 0.16.1 (Cheng *et al.* 2021) in HiFi-only mode with default

137 parameters. We also ran Hifiasm in trio-binning mode, which leverages short-read data from the

138 reference individual's parents to generate haplotype-resolved assemblies. We prepared the
139 maternal and paternal reads by trimming adapters and filtering for quality with fastp v. 0.21.0
140 (Chen *et al.* 2018), merging paired-end reads with PEAR v. 0.9.11 (Zhang *et al.* 2014a), and
141 building a k-mer hash table for each set of reads using yak v. 0.1 (Li 2020). We compared the
142 quality and contiguity of the four draft assemblies (primary, alternate, maternally-resolved
143 haplotype, paternally-resolved haplotype) with Quast v. 5.0.2 (Mikheenko *et al.* 2018) and
144 BUSCO v. 5.2.2 (using the aves_odb10 and eukaryote_odb10 databases; Manni *et al.* 2021) and
145 moved forward with the most contiguous assembly (the primary assembly). To further scaffold
146 the genome, we used the 95.7 Gb of Hi-C reads generated by Dovetail Genomics for the v2
147 Florida Scrub-Jay genome assembly (Driscoll & Beaudry, *et al.* 2021). We used the Arima Hi-C
148 mapping pipeline (https://github.com/ArimaGenomics/mapping_pipeline) to map the paired-end
149 Hi-C reads to the hifiasm primary assembly and SALSA v. 2.3 (Ghurye *et al.* 2017) to join the
150 contigs into scaffolds. We visualized the Hi-C contact map and manually curated the scaffolds to
151 generate a chromosome-level genome assembly using the *juicer.sh*, *run-assembly-visualizer.sh*,
152 and *run-asm-pipeline-post-review.sh* scripts from the Juicer v. 1.6 pipeline (Durand *et al.* 2016).
153 To further improve contiguity, we ordered and oriented scaffolds given positional evidence from
154 our linkage map using ALLMAPS v. 1.3.7 from the JCVI Utilities Library (Tang *et al.* 2015). If
155 any marker locations in the linkage map conflicted with the ordering of contigs joined during the
156 SALSA or Juicer scaffolding steps, we manually broke those scaffolds in disagreement and
157 iteratively ran ALLMAPS until the genetic and physical positions for each linkage group were in
158 concordance. We next screened the genome for organismal contaminants using the BlobToolKit
159 suite v. 3.1.0 (Challis *et al.* 2020) with the *--busco*, *--hits*, and *--cov* flags, and conducted a
160 BLAST search (BLAST v. 2.10.0+; Camacho *et al.* 2009) against the publicly available Florida

161 Scrub-Jay mitochondrial genome sequence (NCBI accession NC_051467.1) to identify and
162 remove any mitochondrial contaminants in the assembly. Finally, we numbered the linkage
163 groups according to homology with the Zebra finch reference genome (*Taeniopygia guttata*;
164 bTaeGut1.4.pri, NCBI accession GCA_003957565.4). Full descriptions of all software and
165 options used for *de novo* genome assembly are available in Table S1.

166

167 **Sex chromosome identification**

168 We identified Z- and W-linked scaffolds using a two-pronged approach: relative read
169 depth and sequence homology to other bird species. Using whole-genome sequence data from 50
170 Florida Scrub-Jays, 25 male and 25 female, we followed the basic methodology from the findZX
171 pipeline (Sigeman *et al.* 2022), a computational pipeline for sex chromosome identification. We
172 processed each set of raw reads as follows: 1) trimmed adapter sequences and low-quality reads
173 using Trim Galore (Krueger *et al.* 2023), 2) mapped the raw reads to the genome assembly using
174 BWA-MEM (Li 2013), 3) filtered for read pairs that completely mapped in the expected
175 orientation with a mapping quality greater than 20 using samtools *view* (Danecek *et al.* 2021), 4)
176 marked and removed duplicate reads using sambamba (Tarasov *et al.* 2015), 5) filtered for reads
177 with an edit distance of less than or equal to 2 using bamtools *filter* (Barnett *et al.* 2011), and 6)
178 calculated per-basepair read depth and average read depth per scaffold across the genome,
179 ignoring repetitive and low complexity regions, using a custom Bash script and samtools *mpileup*
180 (Danecek *et al.* 2021). We then compared the average read depth of each scaffold between males
181 and females in R using a series of t-tests with significance values Bonferroni-corrected for
182 multiple comparisons. We putatively assigned scaffolds with significantly different average read
183 depths as Z-linked if read depth was higher in males than in females and W-linked if read depth

184 was higher in females than in males. We confirmed sex chromosome assignments by aligning
185 each putatively sex-linked scaffold to its appropriate sex chromosome in the Zebra finch
186 reference genome and checking for sequence homology. As an additional check, we aligned W-
187 linked scaffolds to the paternally-resolved haplotype assembly to confirm that they are missing
188 from the male (ZZ) assembly. Finally, we labeled scaffolds as Z-linked or W-linked if they
189 yielded both a significant t-test and displayed sequence homology to the Zebra finch sex
190 chromosomes. Full software parameters are available in Table S1.

191

192 Genome annotation

193 *Repetitive element annotation.* To annotate repetitive content across the genome, we first
194 constructed a custom repeat library for the Florida Scrub-Jay using RepeatModeler v. 2.0.4
195 (Flynn *et al.* 2020) with the *-LTRStruct* flag. We then merged this library with a curated avian
196 repeat library (Peona *et al.* 2021b) and a curated repeat library of the closely-related Steller's Jay
197 (*Cyanocitta stelleri*; Benham *et al.* 2023). We used RepeatMasker v. 4.1.4 (Smit *et al.* 2013) to
198 identify repetitive regions across the genome with the *-s* and *-xsmall* flags to implement a slow
199 search and softmask the genome, respectively. To assess how sequencing technologies (*i.e.*,
200 short-read versus long-read) impacted repeat annotation, we compared the total counts and
201 median lengths of transposable element (TE) superfamilies (Kapitonov and Jurka 2008) across
202 the v2 and v3 assemblies using Wilcoxon rank sum tests.

203 *Gene prediction and functional annotation.* Robust and highly confident gene prediction
204 leverages both RNA-seq and protein data. As such, we used the BRAKER pipeline v. 3.0.6,
205 which integrates both types of data to train and execute the GeneMark-ETP and AUGUSTUS
206 gene prediction tools (Stanke *et al.* 2006, 2008; Gotoh 2008; Iwata and Gotoh 2012; Buchfink *et*

207 *al.* 2015; Hoff *et al.* 2016, 2019; Kovaka *et al.* 2019; Pertea and Pertea 2020; Brůna *et al.* 2021;
208 Bruna *et al.* 2024). We obtained trimmed and filtered 2x101bp RNA-seq reads from liver, heart,
209 and kidney samples from one male and one female, as well as ovary samples from the female
210 (Driscoll & Beaudry, *et al.* 2021). Next, we used STAR v. 2.7.3 (Dobin *et al.* 2013) to align the
211 RNA-seq reads to the softmasked genome assembly and Picard v. 2.27.4 (Broad Institute 2019)
212 to assign read groups to each sample. We then executed BRAKER with the softmasked genome,
213 aligned RNA-seq reads, and the *Vertebrata* protein sequence database from OrthoDB v.11
214 (Kuznetsov *et al.* 2023) as input data. We used InterProScan v. 5.65-97.0 (Jones *et al.* 2014) and
215 a protein BLAST search against the Swiss-Prot database (The UniProt Consortium 2019) to
216 assign functional annotations to the resulting gene set. Finally, we combined the outputs of
217 BRAKER and InterProScan into a consensus gene annotation using the AGAT v. 1.2.0 suite of
218 tools (Dainat 2023). Full descriptions of all software and options used for genome annotation are
219 available in Table S1.

220

221 Genome completeness assessment

222 We used QUAST to calculate basic assembly quality statistics and BUSCO to assess
223 expected gene content and completeness across the genome (as above). To explore synteny
224 across the Aves group, we used minimap2 v. 2.26 (Li 2018) to generate whole genome-whole
225 genome alignments of our assembly with publicly available Zebra finch, chicken (*Gallus gallus*;
226 GGswu, NCBI accession GCA_024206055.2), New Caledonian crow (*Corvus monedulaoides*;
227 bCorMon1.pri, NCBI accession GCA_009650955.1), and the closely related California Scrub-
228 Jay (*Aphelocoma californica*; bAphCal1.0.hap1, NCBI accession GCA_028536675.1) genomes.
229 We filtered for primary alignments with alignment lengths > 10 kB and mapping quality > 40.

230

231 **RESULTS AND DISCUSSION**

232 Linkage map

233 Linkage map construction initially assigned 3,182 SNPs to 36 linkage groups in the pre-
234 framework map. After expanding linkage analysis to the full SNP dataset, we assigned 12,151
235 SNPs to 41 linkage groups. We proceeded to build linkage maps for the 34 linkage groups that
236 contained more than 5 markers (Figure 2). Our framework map with marker order supported by
237 LOD > 5 consists of 4,468 SNPs with a total sex-averaged autosomal genetic map length of
238 2446.78 cM and mean genetic distance between markers of 0.56 cM (\pm 1.33 cM). The female
239 and male autosomal map lengths were 2373.56 cM and 2567.09 cM, respectively (Figure 2). We
240 include the full linkage map in Table S2.

241

242 Genome sequencing and assembly

243 PacBio HiFi long-read sequencing yielded 84 Gb of raw read data, with a mean read
244 length of 14.55 Kb. We created 4 draft assemblies with hifiasm: primary, alternate, maternally-
245 resolved haplotype, and paternally-resolved haplotype. We moved forward with the primary
246 assembly, as it was the most contiguous (L50/N50 of 18 contigs/17.7 Mb) and had the highest
247 BUSCO scores of the three draft assemblies (97.1% completeness; Table S1). Scaffolding with
248 SALSA and Juicer generated an assembly with 699 scaffolds and an L50/N50 of 9
249 scaffolds/33.36 Mb (Figure S1). Linkage map-aided scaffolding with ALLMAPS identified 34
250 linkage groups. Of these linkage groups, 31 (including the Z) were associated with complete
251 chromosomes previously identified in v2 of the Florida Scrub-Jay genome (Driscoll & Beaudry,
252 *et al.* 2021). The remaining 3 linkage groups were newly-assembled chromosomes with sequence

253 homology to chromosomes 30, 31, and 34 in the Zebra finch (Figure 3). Our whole genome
254 assembly displayed broad mapping synteny with other bird genomes, with 81%, 81.5%, 83.7%,
255 and 42.2% of the Florida Scrub-Jay genome aligned to Zebra finch, New Caledonian crow,
256 California Scrub-Jay, and chicken, respectively. As expected, the whole-genome alignment with
257 the most distantly related chicken yielded the most rearrangements and sequence differences,
258 while the alignment with the congeneric California Scrub-Jay yielded the fewest (Figure S2).

259 Next, we identified sex-linked scaffolds by comparing average read coverage per scaffold
260 across 25 male and 25 female Florida Scrub-Jays. We found 17 scaffolds that significantly
261 differed in coverage between males and females. Due to their small size, we were only able to
262 confirm 7 of these scaffolds, 3 Z-linked and 4 W-linked, as homologous to Zebra finch sex
263 chromosome sequence (Figure 3, 4). The largest Z-linked scaffold, which corresponds to the Z
264 linkage group, aligned to ~99% of the Zebra finch Z chromosome (Figure 3). The largest W-
265 linked scaffold was equal in size to the entire Zebra finch W chromosome (~21 Mb), but the 3
266 additional W-linked scaffolds added 15.8 Mb in sequence, yielding a total of 36.8 Mb of
267 sequence identified as part of the Florida Scrub-Jay W chromosome (Figure 3). Finally, we
268 mapped all W-linked scaffolds onto the paternally-resolved haplotype assembly. After filtering
269 using the scheme described previously, we yielded no alignments, further confirming the W
270 assignment of these scaffolds. At the end of these analyses, we labeled the largest Z-linked
271 scaffold as the Z chromosome, the 2 additional Z-linked scaffolds as unlocalized Z sequence, and
272 the 4 W-linked scaffolds as unlocalized W sequence.

273 During decontamination screening with Blob toolkit, one scaffold was identified as
274 belonging to a non-Chordate (specifically, to *Drosophila melanogaster* in Arthropoda; Figure
275 S3); however, we believe this result is a computational artifact because the BLAST hits had low

276 percent identity ($pident = 76\text{-}77\%$) and represented a very low percentage ($\sim 3.3\%$) of the total
277 scaffold length. We therefore retained this scaffold in the final genome assembly. Our final
278 genome assembly is 1.32 Gb long and consists of 660 scaffolds, 87.6% of which belonged to 33
279 named autosomes and the sex chromosomes, with an L50/N50 of 7 scaffolds/88.05 Mb, an
280 average depth of 63x, and a BUSCO completeness score of 97.1% with respect to the
281 aves_odb10 database (Table 1). These quality measures are similar to those of other published
282 genome assemblies in Corvidae and Passeriformes (Table 2). The Florida Scrub-Jay has the
283 longest genome amongst the species considered, and is comparable in length to the more closely-
284 related California Scrub-Jay (1.35 Gb; DeRaad *et al.* 2023).

285

286 Genome annotation

287 *Repetitive content.* We identified 247 Mb of interspersed repeats throughout the genome,
288 comprising 18.71% of the total genome length (Figure 5A). Repetitive content of the v3 genome
289 was more than double that of the v1 and v2 assemblies, which both had an estimated interspersed
290 repeat content of 8.7% (Table S4). The new v3 assembly added \sim 155 Mb of identified repetitive
291 content and yielded more long interspersed nuclear elements (LINEs), long tandem repeats
292 (LTRs), non-LTR retroelements (*e.g.*, short interspersed nuclear elements (SINEs)), satellite
293 sequences, simple repeats, and unclassified repetitive elements (Figure S4A). This increase in
294 repetitive content between our long-read (v3) and short-read (v2) genome assemblies matches
295 similar patterns observed in sparrows (Benham *et al.* 2023b). Avian genomes have long been
296 thought to have low repeat content (< 10%) (Ellegren 2010; Zhang *et al.* 2014b), but genomes
297 assembled with new long-read sequencing technologies are indicating that repeat content in bird
298 genomes has previously been underestimated.

299 The median length of all TE superfamilies differed significantly between the v2 and v3
300 assemblies: long-read sequencing assembled, on average, longer house RNA, satellite, and
301 simple repeat elements (Figure S4B). These results highlight the effectiveness of long-read
302 sequencing technology in assembling both shorter and longer repetitive elements. The most
303 common element across the genome was LTR retrotransposons (14.79%) followed by LINEs
304 (4.17%) (Figure 5), aligning with patterns seen in other avian genomes, particularly amongst
305 songbirds (Kapusta and Suh 2017; Boman *et al.* 2019; Weissensteiner *et al.* 2020). The W-linked
306 scaffold was a strong outlier in repetitive content, with 76.6% of the sequence characterized as
307 interspersed repeats spanning the entire chromosome (Figure S5). The majority of these elements
308 were classified as LTRs, supporting the role of the W chromosome as a haven for repetitive
309 content, particularly long LTR elements, in birds (Peona *et al.* 2021a, 2021b).

310 *Gene content.* We annotated a total number of 17,812 genes throughout the genome, with
311 a mean gene length of 23.1 Kb and a mean of 11.8 exons per gene (Table 2). Of the identified
312 genes, 92.5% were annotated with functional information and 84.3% had an associated gene
313 ontology term. BUSCO completeness of the transcriptome was 95.5% for the *Aves* database and
314 98.4% for the *Eukaryota* database. Mean gene length, mean number exons per gene, and all other
315 annotation quality measures are comparable to that of other similar avian species (Table 2).
316 Notably, we annotated the greatest number of genes (17,812) amongst the species considered
317 (Table 2).

318

319 CONCLUSION

320 We report a high-quality genome assembly, associated annotation, and a linkage map for
321 the Florida Scrub-Jay. Using a combination of long-read sequencing, Hi-C data, and our linkage

322 map, we generated a highly contiguous genome assembly, with a size of 1.32 Gb, an N50 of
323 88.05 Mb, and a BUSCO completeness score of 97.1% (Table 1). Additionally, we provide the
324 first assembly of the W chromosome in this species, as well as three newly identified
325 chromosomes. This annotated genome assembly and linkage map will facilitate more detailed
326 genetic analyses, such as the exploration of haplotype dynamics across space and time and the
327 genetic architecture of fitness, and open the door for new and exciting questions about the
328 biology, ecology, and evolution of this Federally Threatened species.

329

330 **DATA AVAILABILITY**

331 The genome assembly, annotation, and associated raw data for this project are available
332 on NCBI: accession X (pending), BioProject PRJNA1076903, BioSample SAMN39956395. All
333 associated code and data are available at github.com/faye-romero/FSJ-genome.

334

335 **ACKNOWLEDGMENTS**

336 Reed Bowman (1958-2023; Avian Ecology Program, Archbold Biological Station,
337 Venus, FL 33960) was a co-author on this project. We would like to thank the Center for
338 Integrated Research Computing at the University of Rochester for their technical expertise, Tim
339 Sackton for sharing advice and comparative genomic resources, Emiliano Martí for assistance
340 with the genome annotation, and the Chen lab for additional support.

341

342 **FUNDING**

343 Funding provided by the National Science Foundation (NSF) (grant DEB-1257628) and
344 the Cumming Foundation. F.G.R. was supported by a National Institute of Health (NIH) grant to

345 N.C. (1R35GM133412) and a NSF Graduate Research Fellowship (DGE-1939268). F.E.G.B.
346 was supported by the aforementioned NIH grant to N.C. and a NSF Postdoctoral Research
347 Fellowship (2109639).

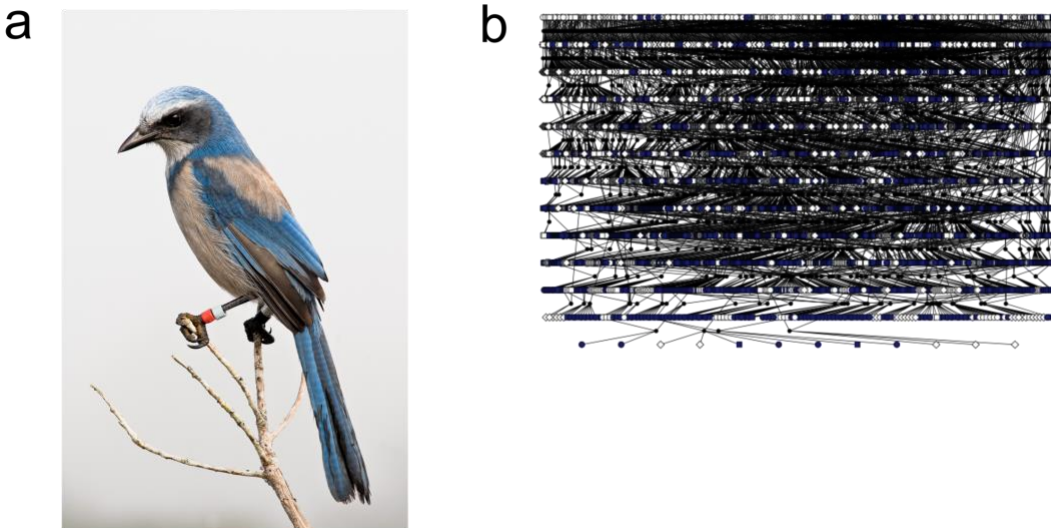
348

349 **CONFLICT OF INTEREST**

350 The authors declare no competing interests.

351

352 **FIGURES**

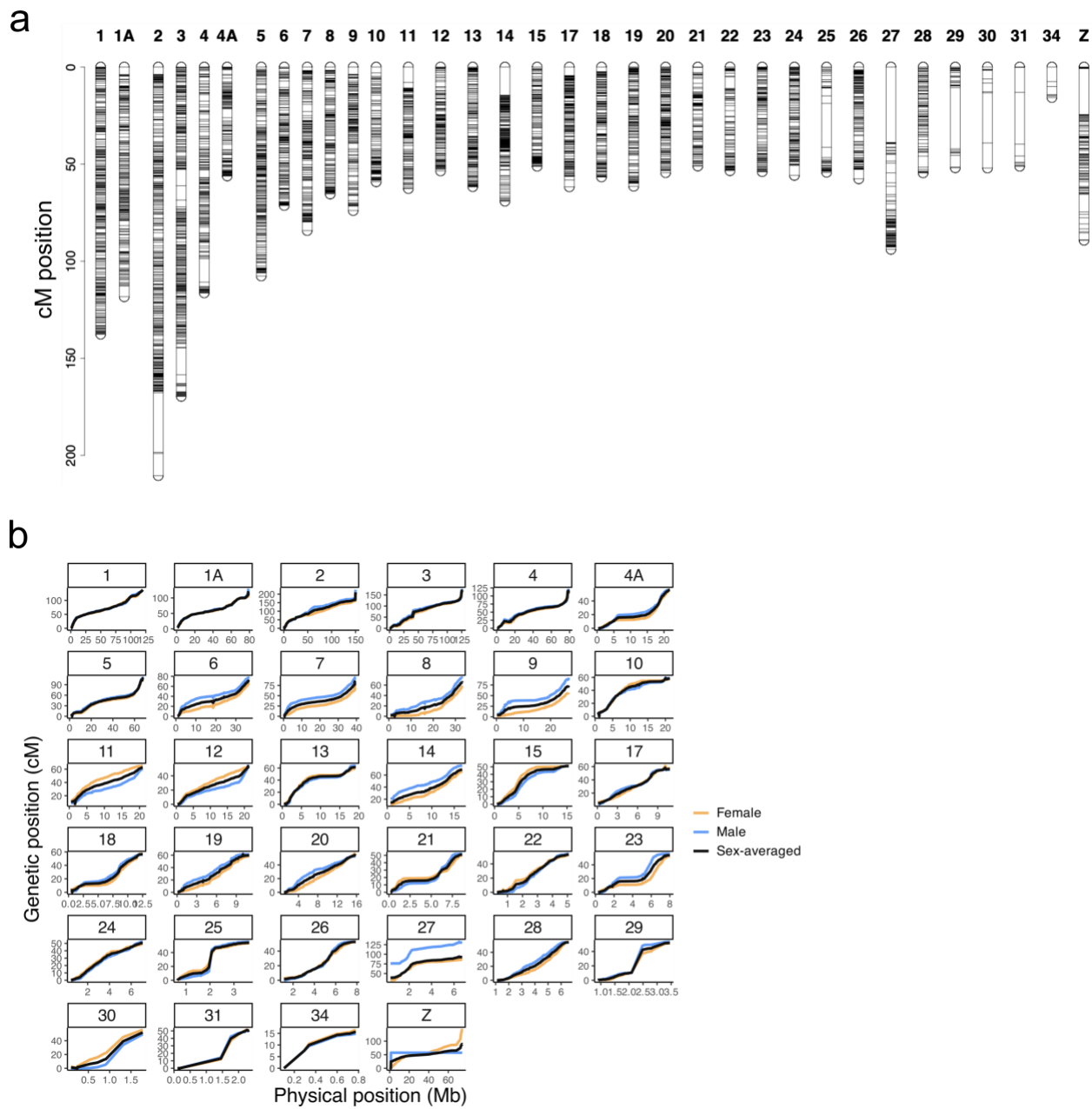


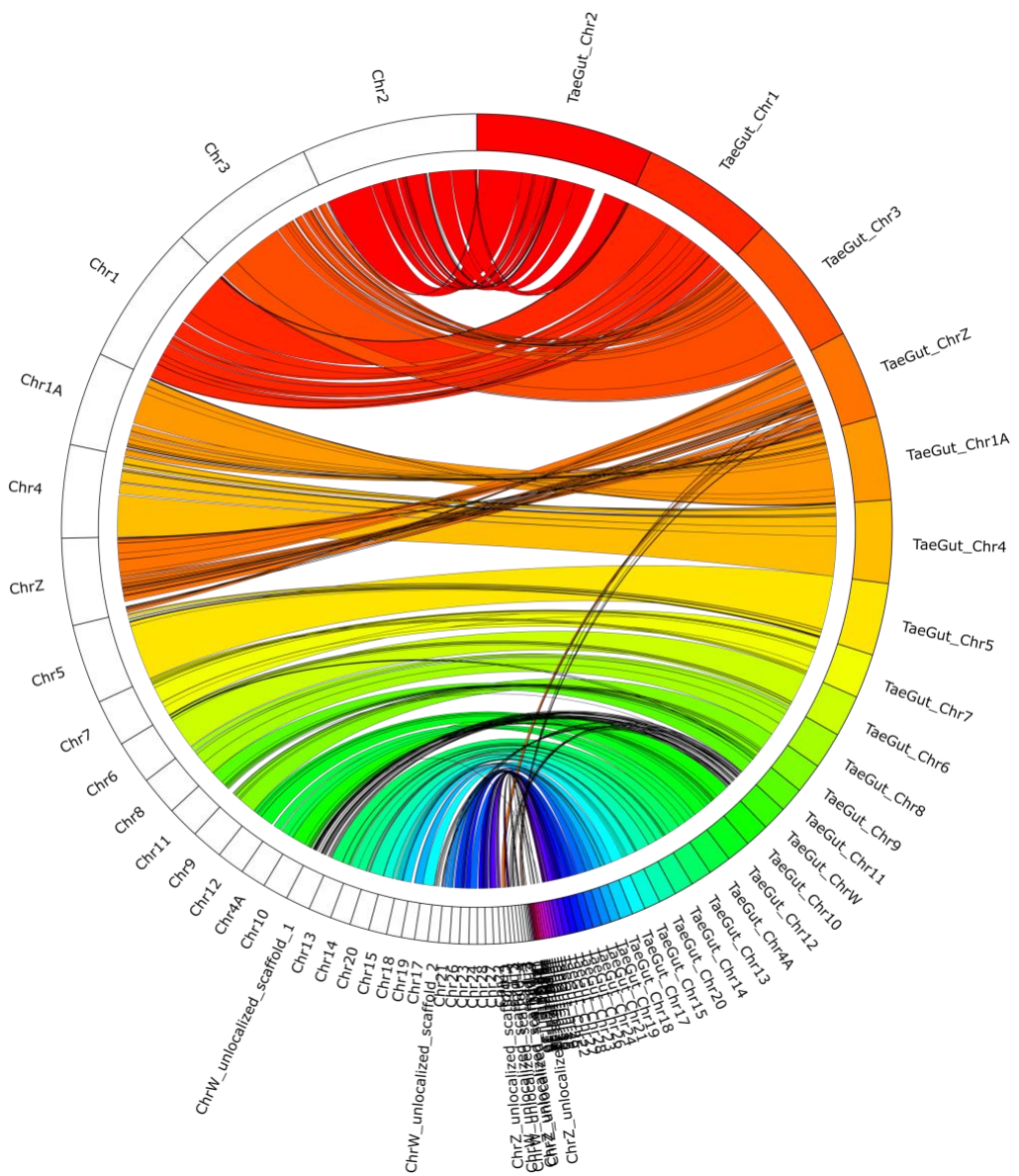
353

354 **Figure 1.** Image and population pedigree of the Florida Scrub-Jay (*Aphelocoma coerulescens*).

355 (A) A banded Florida Scrub-Jay from the long-term demographic study at Archbold Biological
356 Station. Photo courtesy of Reed Bowman. (B) The population pedigree for Florida Scrub-Jays at
357 Archbold Biological Station from 1969-2013. Blue symbols indicate individuals who have been
358 genotyped. N ~ 14,000.

359

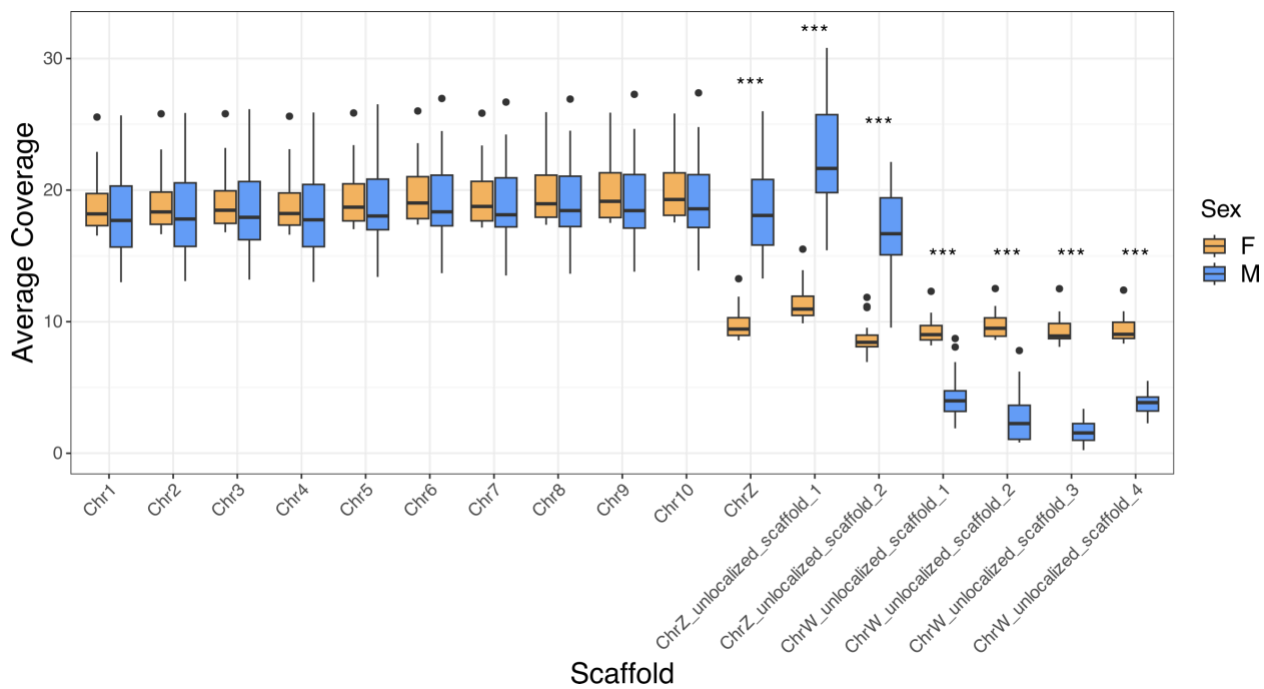




367

368 **Figure 3.** Sequence homology between the Florida Scrub-Jay and the Zebra finch (*Taeniopygia*
369 *guttata*; bTaeGut1.4.pri). The outer ring represents genome sequence divided into
370 chromosomes/scaffolds: white bars on the left represent Florida Scrub-Jay scaffolds and colored
371 bars on the right represent Zebra finch scaffolds, with colored ribbons showing sequence
372 alignment. For clarity, we filtered for alignments > 100kb. We created these plots with Circos v.
373 0.69-9 (Krzywinski *et al.* 2009) with code adapted from the online tutorial
374 <https://bioinf.cc/misc/2020/08/08/circos-ribbons.html>.

375

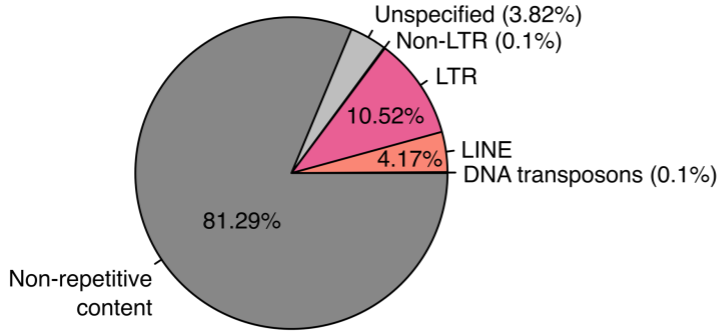


376

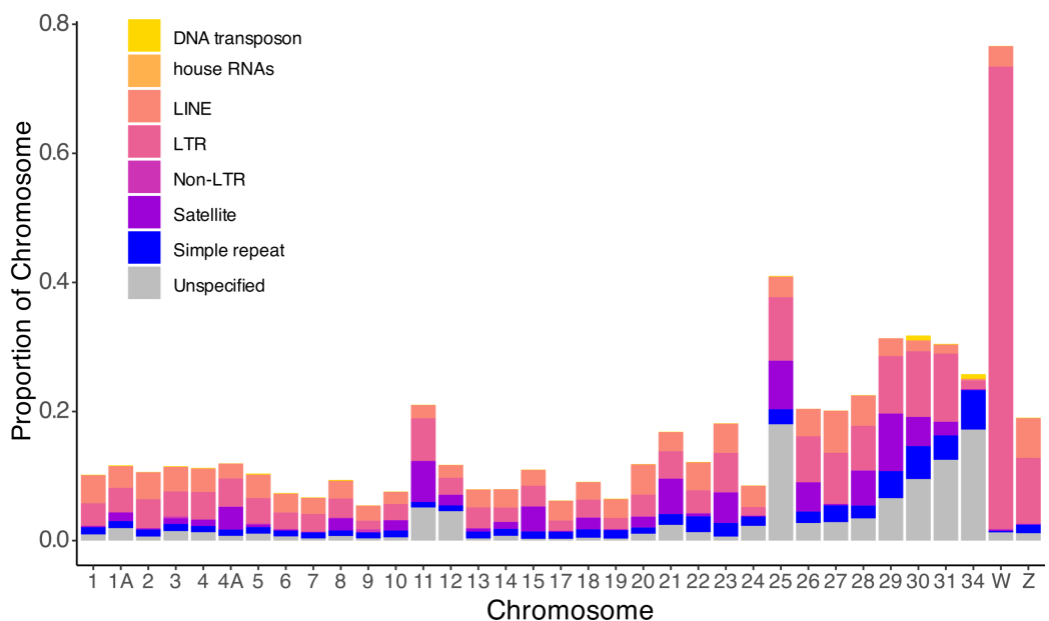
377 **Figure 4.** Average read depth of sex-linked scaffolds in 25 female (yellow) and male (blue)
378 Florida Scrub-Jays. We include the first 10 autosomes for comparison. W-linked scaffolds show
379 approximately twice the coverage in females when compared to males, while Z-linked scaffolds
380 show approximately twice the coverage in males when compared to females. Scaffolds with
381 significantly different average read depths from a t-test are indicated as follows: * = $p < 2.26 \times 10^{-5}$, ** = $p < 2.26 \times 10^{-6}$, *** = $p < 2.26 \times 10^{-7}$ (p-values were Bonferroni-corrected for 442
382 comparisons).

384

a



b



385

386 **Figure 5.** Repeat annotation of the Florida Scrub-Jay genome. (A) Summary of interspersed
387 repeat content across the whole genome. (B) Repetitive content of each chromosome, colored by
388 transposable element superfamily (Kapitonov and Jurka 2008).

389

390 **TABLES**

391

	Hifiasm	+ SALSA2	+ Juicer manual curation	+ ALLMAPS
Total length (bp)	1322553486	1322602486	1322601186	1322605086
Number of contigs/scaffolds	783	699	699	660
N50 (Mb)	17.71	33.36	33.36	68.05
L50	18	9	9	7
Longest contig/scaffold (Mb)	93.47	124.80	124.80	150.66
Number of N's per 100 kbp	0.00	3.70	3.61	3.90
BUSCO scores (%) (Aves; n = 8338)	C: 97.1 S: 96.5 D: 0.6 F: 0.5 M: 2.4	C: 97.0 S: 96.4 D: 0.6 F: 0.5 M: 2.5	C: 97.2 S: 96.5 D: 0.7 F: 0.6 M: 2.2	C: 97.1 S: 96.4 D: 0.7 F: 0.6 M: 2.3
BUSCO scores (%) (Eukaryota; n = 255)	C: 98.8 S: 97.6 D: 1.2 F: 0.8 M: 0.4	C: 98.8 S: 98.0 D: 0.8 F: 0.8 M: 0.4	C: 98.8 S: 97.6 D: 1.2 F: 0.8 M: 0.4	C: 99.2 S: 98.0 D: 1.2 F: 0.4 M: 0.4

392

393 **Table 1.** Basic assembly statistics for each step of the v3 Florida Scrub-Jay genome assembly.

394 The Hifiasm column reports statistics for contigs, while all other columns report statistics for
395 scaffolds. The *Aves* row of BUSCO (Benchmarking Universal Single-Copy Orthologs) scores
396 uses the *aves_odb10* (2024-01-08) database with 8338 BUSCOs available. The *Eukaryota* row of
397 BUSCO scores uses the *eukaryote_odb10* (2024-01-08) database with 255 BUSCOs available.
398 BUSCO parameters are as follows: C: Complete, S: Complete and single-copy, D: Complete and
399 duplicated, F: Fragmented, M: Missing (Manni *et al.* 2021).

	Florida Scrub-Jay	New Caledonian crow	Hawaiian crow	Hooded crow	Collared flycatcher	Zebra finch
Genome assembly length (Gb)	1.3	1.1	1.2	1.0	1.1	1.22
Contig N50 (Mb)	17.7	11.5	23.1	8.6	0.41	0.038
No. of genes	17,812	16,167	16,414	14,435	16,763	17,561
Mean gene length (bp)	23,127	36,436	35,242	37,961	31,394	26,458
Number of CDS	26,521	43,047	43,147	36,899	16,763	17,561
Mean length of CDS (bp)	1,912	2,293	2,332	2,275	1,942	1,677
No. of exons	311,707	638,785	648,529	555,077	189,043	171,767
Mean exon length (bp)	162	291	283	293	253	255
Mean no. exons per gene	11.8	14.1	14.3	14.3	12.2	10.3
No. of introns	285,186	563,402	573,808	490,050	171,236	153,909
Genome BUSCO scores (%) (Aves; n = 8338)	C: 97.1 S: 96.4 D: 0.7 F: 0.6 M: 2.3	C: 96.8 S: 96.3 D: 0.5 F: 0.5 M: 2.7	C: 97.3 S: 96.8 D: 0.5 F: 0.5 M: 2.2	C: 94.8 S: 94.4 D: 0.4 F: 0.5 M: 4.6	C: 96.5 S: 96 D: 0.5 F: 0.8 M: 2.7	C: 93.8 S: 91.9 D: 1.9 F: 2.3 M: 3.9

400

401 **Table 2.** Summary statistics for the Florida Scrub-Jay (*A. coerulescens*) genome and annotation

402 compared to other similar bird species in Corvidae and Passeriformes (New Caledonian crow,

403 *Corvus monedula*; Hawaiian crow, *Corvus hawaiiensis*; Hooded crow, *Corvus cornix*;

404 Collared fly catcher, *Ficedula albicollis*; Zebra finch, *Taeniopygia guttata*). We calculated

405 annotation statistics for each species by inputting their publicly available annotation files (GFF)

406 into the AGAT toolkit script *agat_sp_statistics.pl* (Dainat 2023). Note that genome assembly

407 length, contig N50, and genome BUSCO scores are genome summary statistics, while all other

408 statistics are gene annotation summary statistics. BUSCO parameters are as follows: C:

409 Complete, S: Complete and single-copy, D: Complete and duplicated, F: Fragmented, M:

410 Missing (Manni *et al.* 2021). Modified from (Peona *et al.* 2023).

411

412 REFERENCES

413 Aguillon, S. M., J. W. Fitzpatrick, R. Bowman, S. J. Schoech, A. G. Clark *et al.*, 2017
414 Deconstructing isolation-by-distance: The genomic consequences of limited dispersal.
415 PLOS Genetics 13: e1006911.
416 Barnett, D. W., E. K. Garrison, A. R. Quinlan, M. P. Strömberg, and G. T. Marth, 2011
417 BamTools: a C++ API and toolkit for analyzing and managing BAM files.
418 Bioinformatics 27: 1691–1692.
419 Benham, P. M., C. Cicero, D. A. DeRaad, J. E. McCormack, R. K. Wayne *et al.*, 2023a A highly
420 contiguous reference genome for the Steller’s jay (*Cyanocitta stelleri*). Journal of
421 Heredity 114: 549–560.
422 Benham, P. M., C. Cicero, M. Escalona, E. Beraut, C. Fairbairn *et al.*, 2023b Remarkably high
423 repeat content in the genomes of sparrows: the importance of genome assembly
424 completeness for transposable element discovery. 2023.10.26.564301.
425 Boman, J., C. Frankl-Vilches, M. da Silva dos Santos, E. H. C. de Oliveira, M. Gahr *et al.*, 2019
426 The Genome of Blue-Capped Cordon-Bleu Uncovers Hidden Diversity of LTR
427 Retrotransposons in Zebra Finch. Genes (Basel) 10: 301.
428 Boughton, D. R. K., and D. R. Bowman, 2011 State wide assessment of Florida Scrub-Jays on
429 managed areas: A comparison of current populations to the results of the 1992-93 survey.
430 Breininger, D. R., M. A. Burgman, and B. M. Stith, 1999 Influence of Habitat Quality,
431 Catastrophes, and Population Size on Extinction Risk of the Florida Scrub-Jay. Wildlife
432 Society Bulletin (1973-2006) 27: 810–822.

433 Breininger, D. R., and G. M. Carter, 2003 TERRITORY QUALITY TRANSITIONS AND
434 SOURCE–SINK DYNAMICS IN A FLORIDA SCRUB-JAY POPULATION.
435 Ecological Applications 13: 516–529.

436 Broad Institute, 2019 Picard Toolkit.

437 Brůna, T., K. J. Hoff, A. Lomsadze, M. Stanke, and M. Borodovsky, 2021 BRAKER2: automatic
438 eukaryotic genome annotation with GeneMark-EP+ and AUGUSTUS supported by a
439 protein database. NAR Genomics and Bioinformatics 3: lqaa108.

440 Bruna, T., A. Lomsadze, and M. Borodovsky, 2024 GeneMark-ETP: Automatic Gene Finding in
441 Eukaryotic Genomes in Consistency with Extrinsic Data. 2023.01.13.524024.

442 Buchfink, B., C. Xie, and D. H. Huson, 2015 Fast and sensitive protein alignment using
443 DIAMOND. Nat Methods 12: 59–60.

444 Camacho, C., G. Coulouris, V. Avagyan, N. Ma, J. Papadopoulos *et al.*, 2009 BLAST+:
445 architecture and applications. BMC Bioinformatics 10: 421.

446 Challis, R., E. Richards, J. Rajan, G. Cochrane, and M. Blaxter, 2020 BlobToolKit – Interactive
447 Quality Assessment of Genome Assemblies. G3 Genes|Genomes|Genetics 10: 1361–
448 1374.

449 Chen, N., E. J. Cosgrove, R. Bowman, J. W. Fitzpatrick, and A. G. Clark, 2016 Genomic
450 Consequences of Population Decline in the Endangered Florida Scrub-Jay. Current
451 Biology 26: 2974–2979.

452 Chen, N., I. Juric, E. J. Cosgrove, R. Bowman, J. W. Fitzpatrick *et al.*, 2019 Allele frequency
453 dynamics in a pedigreed natural population. Proceedings of the National Academy of
454 Sciences 116: 2158–2164.

455 Chen, S., Y. Zhou, Y. Chen, and J. Gu, 2018 fastp: an ultra-fast all-in-one FASTQ preprocessor.

456 Bioinformatics 34: i884–i890.

457 Cheng, H., G. T. Concepcion, X. Feng, H. Zhang, and H. Li, 2021 Haplotype-resolved de novo

458 assembly using phased assembly graphs with hifiasm. Nat Methods 18: 170–175.

459 Coulon, A., J. W. Fitzpatrick, R. Bowman, and I. J. Lovette, 2010 Effects of habitat

460 fragmentation on effective dispersal of florida scrub-jays: Fragmentation decreases

461 effective dispersal. Conservation Biology 24: 1080–1088.

462 Coulon, A., J. W. Fitzpatrick, R. Bowman, and I. J. Lovette, 2012 Mind the gap: genetic distance

463 increases with habitat gap size in Florida scrub jays. Biology Letters 8: 582–585.

464 Coulon, A., J. W. Fitzpatrick, R. Bowman, B. M. Stith, C. A. Makarewich *et al.*, 2008 Congruent

465 population structure inferred from dispersal behaviour and intensive genetic surveys of

466 the threatened Florida scrub-jay (*Aphelocoma coerulescens*). Molecular Ecology 17:

467 1685–1701.

468 Dainat, J., 2023 AGAT: Another Gff Analysis Toolkit to handle annotations in any GTF/GFF

469 format.

470 Danecek, P., J. K. Bonfield, J. Liddle, J. Marshall, V. Ohan *et al.*, 2021 Twelve years of

471 SAMtools and BCFtools. GigaScience 10: giab008.

472 DeRaad, D. A., M. Escalona, P. Benham, M. P. A. Marimuthu, R. M. Sahasrabudhe *et al.*, 2023

473 De novo assembly of a chromosome-level reference genome for the California Scrub-Jay,

474 *Aphelocoma californica*. Journal of Heredity esad047.

475 Dobin, A., C. A. Davis, F. Schlesinger, J. Drenkow, C. Zaleski *et al.*, 2013 STAR: ultrafast

476 universal RNA-seq aligner. Bioinformatics 29: 15–21.

477 Driscoll, R. M. H., F. E. G. Beaudry, E. J. Cosgrove, R. Bowman, J. W. Fitzpatrick *et al.*, 2021

478 Allele frequency dynamics under sex-biased demography and sex-specific inheritance in

479 a pedigreed population. 2021.10.28.466320.

480 Durand, N. C., M. S. Shamim, I. Machol, S. S. P. Rao, M. H. Huntley *et al.*, 2016 Juicer

481 Provides a One-Click System for Analyzing Loop-Resolution Hi-C Experiments. *Cell*

482 *Syst* 3: 95–98.

483 Ellegren, H., 2010 Evolutionary stasis: the stable chromosomes of birds. *Trends in Ecology &*

484 *Evolution* 25: 283–291.

485 Feng, S., J. Stiller, Y. Deng, J. Armstrong, Q. Fang *et al.*, 2020 Dense sampling of bird diversity

486 increases power of comparative genomics. *Nature* 587: 252–257.

487 Flynn, J. M., R. Hubley, C. Goubert, J. Rosen, A. G. Clark *et al.*, 2020 RepeatModeler2 for

488 automated genomic discovery of transposable element families. *Proceedings of the*

489 *National Academy of Sciences* 117: 9451–9457.

490 Ghurye, J., M. Pop, S. Koren, D. Bickhart, and C.-S. Chin, 2017 Scaffolding of long read

491 assemblies using long range contact information. *BMC Genomics* 18: 527.

492 Gotoh, O., 2008 A space-efficient and accurate method for mapping and aligning cDNA

493 sequences onto genomic sequence. *Nucleic Acids Research* 36: 2630–2638.

494 Green, P., I. Evans, and J. Maddox, 1990 CRI-MAP: Improved.

495 Hoff, K. J., S. Lange, A. Lomsadze, M. Borodovsky, and M. Stanke, 2016 BRAKER1:

496 Unsupervised RNA-Seq-Based Genome Annotation with GeneMark-ET and

497 AUGUSTUS. *Bioinformatics* 32: 767–769.

498 Hoff, K. J., A. Lomsadze, M. Borodovsky, and M. Stanke, 2019 Whole-Genome Annotation
499 with BRAKER, pp. 65–95 in *Gene Prediction: Methods and Protocols*, edited by M.
500 Kollmar. Methods in Molecular Biology, Springer, New York, NY.

501 Iwata, H., and O. Gotoh, 2012 Benchmarking spliced alignment programs including Spaln2, an
502 extended version of Spaln that incorporates additional species-specific features. Nucleic
503 Acids Research 40: e161.

504 Johnston, S. E., C. Bérénos, J. Slate, and J. M. Pemberton, 2016 Conserved Genetic Architecture
505 Underlying Individual Recombination Rate Variation in a Wild Population of Soay Sheep
506 (*Ovis aries*). Genetics 203: 583–598.

507 Jones, P., D. Binns, H.-Y. Chang, M. Fraser, W. Li *et al.*, 2014 InterProScan 5: genome-scale
508 protein function classification. Bioinformatics 30: 1236–1240.

509 Kapitonov, V. V., and J. Jurka, 2008 A universal classification of eukaryotic transposable
510 elements implemented in Repbase. Nat Rev Genet 9: 411–412.

511 Kapusta, A., and A. Suh, 2017 Evolution of bird genomes—a transposon’s-eye view. Annals of
512 the New York Academy of Sciences 1389: 164–185.

513 Kovaka, S., A. V. Zimin, G. M. Pertea, R. Razaghi, S. L. Salzberg *et al.*, 2019 Transcriptome
514 assembly from long-read RNA-seq alignments with StringTie2. Genome Biology 20:
515 278.

516 Krueger, F., F. James, P. Ewels, E. Afyounian, M. Weinstein *et al.*, 2023 Trim Galore.

517 Krzywinski, M. I., J. E. Schein, I. Birol, J. Connors, R. Gascoyne *et al.*, 2009 Circos: An
518 information aesthetic for comparative genomics. Genome Res.

519 Kuznetsov, D., F. Tegenfeldt, M. Manni, M. Seppey, M. Berkeley *et al.*, 2023 OrthoDB v11:
520 annotation of orthologs in the widest sampling of organismal diversity. *Nucleic Acids*
521 *Research* 51: D445–D451.

522 Li, H., 2013 Aligning sequence reads, clone sequences and assembly contigs with BWA-MEM.

523 Li, H., 2018 Minimap2: pairwise alignment for nucleotide sequences. *Bioinformatics* 34: 3094–
524 3100.

525 Li, H., 2020 yak: Yet another k-mer analyzer.

526 Linderroth, T., L. Deaner, N. Chen, R. Bowman, R. Boughton *et al.*, 2023 Translocations spur
527 population growth but exacerbate inbreeding in an imperiled species. 2023.11.11.566550.

528 Liu, X., and M. Grosz, 2006.

529 Manni, M., M. R. Berkeley, M. Seppey, F. A. Simão, and E. M. Zdobnov, 2021 BUSCO Update:
530 Novel and Streamlined Workflows along with Broader and Deeper Phylogenetic
531 Coverage for Scoring of Eukaryotic, Prokaryotic, and Viral Genomes. *Molecular Biology*
532 and Evolution

533 38: 4647–4654.

534 Martin, M., 2011 Cutadapt removes adapter sequences from high-throughput sequencing reads.
535 *EMBnet.journal* 17: 10–12.

536 Mikheenko, A., A. Prjibelski, V. Saveliev, D. Antipov, and A. Gurevich, 2018 Versatile genome
537 assembly evaluation with QUAST-LG. *Bioinformatics* 34: i142–i150.

538 Mumme, R. L., R. Bowman, M. S. Pruett, and J. W. Fitzpatrick, 2015 Natal territory size, group
539 size, and body mass affect lifetime fitness in the cooperatively breeding Florida Scrub-Jay. *The Auk* 132: 634–646.

540 Nguyen, T. N., N. Chen, E. J. Cosgrove, R. Bowman, J. W. Fitzpatrick *et al.*, 2022 Dynamics of
541 reduced genetic diversity in increasingly fragmented populations of Florida scrub
542 jays, *Aphelocoma coerulescens*. *Evolutionary Applications* 15: 1018–1027.

543 Ouellette, L. A., R. W. Reid, S. G. Blanchard, and C. R. Brouwer, 2018 LinkageMapView—
544 rendering high-resolution linkage and QTL maps. *Bioinformatics* 34: 306–307.

545 Peona, V., M. P. K. Blom, L. Xu, R. Burri, S. Sullivan *et al.*, 2021a Identifying the causes and
546 consequences of assembly gaps using a multiplatform genome assembly of a bird-of-
547 paradise. *Molecular Ecology Resources* 21: 263–286.

548 Peona, V., O. M. Palacios-Gimenez, J. Blommaert, J. Liu, T. Haryoko *et al.*, 2021b The avian W
549 chromosome is a refugium for endogenous retroviruses with likely effects on female-
550 biased mutational load and genetic incompatibilities. *Philosophical Transactions of the
551 Royal Society B: Biological Sciences* 376: 20200186.

552 Peona, V., O. M. Palacios-Gimenez, D. Lutgen, R. A. Olsen, N. Alaei Kakhki *et al.*, 2023 An
553 annotated chromosome-scale reference genome for Eastern black-eared wheatear
554 (*Oenanthe melanoleuca*). *G3 Genes|Genomes|Genetics* 13: jkad088.

555 Pertea, G., and M. Pertea, 2020 GFF Utilities: GffRead and GffCompare. *F1000Research* 9:.

556 Sigeman, H., B. Sinclair, and B. Hansson, 2022 Findzx: an automated pipeline for detecting and
557 visualising sex chromosomes using whole-genome sequencing data. *BMC Genomics* 23:
558 328.

559 Smit, A., R. Hubley, and P. Green, 2013 RepeatMasker Open-4.0.

560 Stanke, M., M. Diekhans, R. Baertsch, and D. Haussler, 2008 Using native and syntenically
561 mapped cDNA alignments to improve de novo gene finding. *Bioinformatics* 24: 637–
562 644.

563 Stanke, M., O. Schöffmann, B. Morgenstern, and S. Waack, 2006 Gene prediction in eukaryotes
564 with a generalized hidden Markov model that uses hints from external sources. *BMC*
565 *Bioinformatics* 7: 62.

566 Suh, Y. H., R. Bowman, and J. W. Fitzpatrick, 2022 Staging to join non-kin groups in a classical
567 cooperative breeder, the Florida scrub-jay. *J. Anim. Ecol.* 91: 970–982.

568 Suh, Y. H., M. B. Pesendorfer, A. Tringali, R. Bowman, and J. W. Fitzpatrick, 2020
569 Investigating social and environmental predictors of natal dispersal in a cooperative
570 breeding bird. *Behavioral Ecology* 31: 692–701.

571 Summers, J., E. J. Cosgrove, R. Bowman, J. W. Fitzpatrick, and N. Chen, 2024 Impacts of
572 increasing isolation and environmental variation on Florida Scrub-Jay demography.
573 2024.01.10.575127.

574 Tang, H., X. Zhang, C. Miao, J. Zhang, R. Ming *et al.*, 2015 ALLMAPS: robust scaffold
575 ordering based on multiple maps. *Genome Biology* 16: 3.

576 Tarasov, A., A. J. Vilella, E. Cuppen, I. J. Nijman, and P. Prins, 2015 Sambamba: fast processing
577 of NGS alignment formats. *Bioinformatics* 31: 2032–2034.

578 The UniProt Consortium, 2019 UniProt: a worldwide hub of protein knowledge. *Nucleic Acids*
579 *Research* 47: D506–D515.

580 Thomas, J. A., M. G. Telfer, D. B. Roy, C. D. Preston, J. J. D. Greenwood *et al.*, 2004
581 Comparative Losses of British Butterflies, Birds, and Plants and the Global Extinction
582 Crisis. *Science* 303: 1879–1881.

583 Thorington, K. K., and R. Bowman, 2003 Predation rate on artificial nests increases with human
584 housing density in suburban habitats. *Ecography* 26: 188–196.

585 Treangen, T. J., and S. L. Salzberg, 2012 Repetitive DNA and next-generation sequencing:
586 computational challenges and solutions. *Nat Rev Genet* 13: 36–46.

587 Weissensteiner, M. H., I. Bunikis, A. Catalán, K.-J. Francoijjs, U. Knief *et al.*, 2020 Discovery
588 and population genomics of structural variation in a songbird genus. *Nat Commun* 11:
589 3403.

590 Woolfenden, G. E., and J. W. Fitzpatrick, 1984 *The Florida Scrub Jay: Demography of a*
591 *Cooperatively-Breeding Bird*. Princeton University Press.

592 Zhang, J., K. Kobert, T. Flouri, and A. Stamatakis, 2014a PEAR: a fast and accurate Illumina
593 Paired-End reAd mergeR. *Bioinformatics* 30: 614–620.

594 Zhang, G., C. Li, Q. Li, B. Li, D. M. Larkin *et al.*, 2014b Comparative genomics reveals insights
595 into avian genome evolution and adaptation. *Science* 346: 1311–1320.

596